Harvesting Infrared Photons with Croconate Dyes

Kensuke Takechi[†] and Prashant V. Kamat*[,†,‡]

Radiation Laboratory and Departments of Chemistry and Biochemistry and Chemical & Biomolecular Engineering, University of Notre Dame, Notre Dame, Indiana 46556-5674

Rekha R. Avirah, Kuthanapillil Jyothish, and Danaboyina Ramaiah

Photosciences and Photonics, Chemical Sciences and Technology Division, National Institute for Interdisciplinary Science & Technology (NIIST), Council of Scientific and Industrial Research, Trivandrum 695 019, India

Received July 16, 2007. Revised Manuscript Received October 23, 2007

Excited-state properties of the croconate dyes were investigated with an aim to utilize them as light harvesting assemblies in the infrared (IR) region ($\lambda_{max} \sim 865$ nm and $M^{-1}\ c^{-1} = (1.4-4.2) \times 10^5\ M^{-1}\ s^{-1}$). The excited singlet of the monomeric dye quickly deactivates (lifetime 4−7 ps) without undergoing intersystem crossing to generate triplet. The triplet excited-state produced via triplet–triplet energy transfer method show relatively long life (lifetime 7.2 μs). The dye molecules when deposited as thin film on optically transparent electrodes or on nanostructured TiO_2 film form H-aggregates with a blue-shifted absorption maximum around 660 nm. The excitons formed upon excitation of the dye aggregates undergo charge separation at the TiO_2 and SnO_2 interface. The H-aggregates in the film are photoactive and produce anodic current (IPCE of 1.2% at 650 nm) when employed in a photoelectrochemical cell. Spectroscopic and photoelectrochemical experiments that highlight the usefulness of croconate dyes in IR light harvesting applications are described.

Introduction

Dyes absorbing in the infrared region are important for extending the photoresponse of solar cells as they can harvest low-energy photons that usually goes untapped.[1] Application of such IR dyes is seen in solar cells, photodynamic therapy, nonlinear optics, lasers, and optoelectronic devices.[1–13] Of particular interest are squaraine and croconate dyes (Scheme 1) that exhibit strong absorption in the infrared.[4,5,14] These dye molecules possess donor–acceptor–donor type structure,

Scheme 1. Parent Structure of Croconate Dye

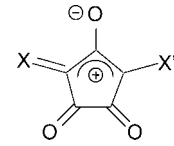

and their absorption in the IR region can be tuned by varying donor moieties. In addition, these dyes also exhibit a strong solvatochromic shift. Carbocyanine dyes are another class of dyes that absorb in the red−infrared region. An interesting aspect of these dye molecules is their ability to undergo intermolecular interaction and produce H-type and J-type aggregates.[15–23] By making use of this property, we have demonstrated the possibility of tuning the absorptive range of a photoelectrochemical cell.[24,25]

Earlier, we have undertaken detailed photophysical and photochemical investigations to probe the excited-state

* Address correspondence to this author: e-mail pkamat@nd.edu.
† Radiation Laboratory.
‡ Departments of Chemistry and Biochemistry and Chemical & Biomolecular Engineering.

(1) Kamat, P. V. *J. Phys. Chem. C* **2007**, *111*, 2834.
(2) Ramaiah, D.; Eckert, I.; Arun, K. T.; Weidenfeller, L.; Epe, B. *Photochem. Photobiol.* **2002**, *76*, 672.
(3) Ramaiah, D.; Joy, A.; Chandrasekhar, N.; Eldho, N. V.; Das, S.; George, M. V. *Photochem. Photobiol.* **1997**, *65*, 783.
(4) Law, K. Y. *Chem. Rev.* **1993**, *93*, 449.
(5) Fabian, J.; Zahradnik, R. *Angew. Chem., Int. Ed. Engl.* **1989**, *28*, 677.
(6) Spitler, M.; Parkinson, B. A. *Langmuir* **1986**, *2*, 549.
(7) Altobello, S.; Argazzi, R.; Caramori, S.; Contado, C.; Da Fre, S.; Rubino, P.; Chone, C.; Larramona, G.; Bignozzi, C. A. *J. Am. Chem. Soc.* **2005**, *127*, 15342.
(8) Wang, X. J.; Perzon, E.; Delgado, J. L.; de la Cruz, P.; Zhang, F. L.; Langa, F.; Andersson, M.; Inganas, O. *Appl. Phys. Lett.* **2004**, *85*, 5081.
(9) Rand, B. P.; Xue, J. G.; Yang, F.; Forrest, S. R. *Appl. Phys. Lett.* **2005**, *87*, 233508.
(10) Xue, J. G.; Uchida, S.; Rand, B. P.; Forrest, S. R. *Appl. Phys. Lett.* **2004**, *85*, 5757.
(11) Arunkumar, E.; Fu, N.; Smith, B. D. *Chem.—Eur. J.* **2006**, *12*, 4684.
(12) Arunkumar, E.; Forbes, C. C.; Noll, B. C.; Smith, B. D. *J. Am. Chem. Soc.* **2005**, *127*, 3288.
(13) Arunkumar, E.; Sudeep, P. K.; Kamat, P. V.; Noll, B. C.; Smith, B. D. *New J. Chem.* **2007**, *31*, 677.
(14) Fabian, J.; Nakazumi, H.; Matsuoka, M. *Chem. Rev.* **1992**, *92*, 1197.
(15) Serpone, N.; Sahyun, M. R. V. *J. Phys. Chem.* **1994**, *98*, 734.
(16) Soper, S. A.; Mattingly, Q. L. *J. Am. Chem. Soc.* **1994**, *116*, 3744.
(17) Chen, S.-Y.; Horng, M.-L.; Quitevis, E. L. *J. Phys. Chem.* **1989**, *93*, 3683.
(18) Tani, T.; Suzumoto, T.; Kemnitz, K.; Yoshihara, K. *J. Phys. Chem.* **1992**, *96*, 2778.
(19) Noukakis, D.; Van der Auweraer, M.; Toppet, S.; De Schryver, F. C. *J. Phys. Chem.* **1995**, *99*, 11860.
(20) Chibisov, A. K.; Zakharova, G. V.; Goerner, H.; Sogulyaev, Y. A.; Mushkalo, I. L.; Tolmachev, A. I. *J. Phys. Chem.* **1995**, *99*, 886.
(21) Trosken, B.; Wiilig, F.; Schwarzburg, K.; Ehret, A.; Spitler, M. *J. Phys. Chem.* **1995**, *99*, 5152.
(22) Yonezawa, Y.; Ishizawa, H. *J. Lumin.* **1996**, *69*, 141.
(23) Arun, K. T.; Epe, B.; Ramaiah, D. *J. Phys. Chem. B* **2002**, *106*, 11622.
(24) Takechi, K.; Sudeep, S.; Kamat, P. V. *J. Phys. Chem. B* **2006**, *110*, 16169.
(25) Sudeep, P. K.; Takechi, K.; Kamat, P. V. *J. Phys. Chem. C* **2007**, *111*, 488.

10.1021/cm7018668 CCC: $40.75
Published on Web 12/12/2007

Scheme 2. Structures of the Croconate Dyes Employed in the Present Investigation

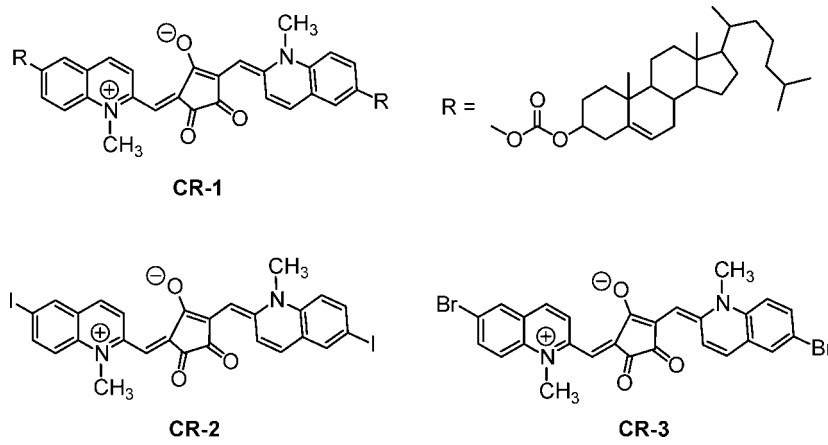

behavior of several squaraine[13,26–32] and carbocyanine dyes[25,33] and their ability to sensitize TiO_2 particles.[34] The photochemical investigation of IR dyes is often limited because of the short-lived singlet excited state (usually a few picoseconds). We have now investigated the excited-state properties of a new class of croconate dyes (Scheme 2) using femtosecond transient absorption spectroscopy.

In recent years effort has been made to explore the structural and optical properties of croconate dyes.[35–41] Usually, the small HOMO–LUMO gap of IR-absorbing dyes is attained by means of extended π-conjugation. A recent study shows that with simple structural manipulation one can achieve absorption in the 1.1 μm region.[36] Bhanuprakash and co-workers[40,41] have carried out structural analysis and explored the role of oxyallyl substructures in tuning the absorption and hyperpolarizability of croconate dyes. Initial studies on the electrochemical and photoelectrochemical aspects of simple croconate dyes have pointed out their usefulness in light energy conversion applications.[42,43] Photophysical and photoelectrochemical properties of newly synthesized croconate dyes (Scheme 2) presented in the present study should provide further insight into their excited-state behavior and limitations in light energy harvesting applications.

Experimental Section

Materials and Methods. The materials used were of the highest quality and used as received. All melting points are uncorrected and were determined on a Mel-Temp II melting point apparatus.[44,45] The IR spectra were recorded on a Perkin-Elmer model 882 infrared spectrometer. The ^{1}H and ^{13}C NMR spectra were measured on a 300 MHz Bruker advanced DPX spectrometer. All the solvents used were purified and distilled before use. Absorption spectra were recorded using a Varian model CARY 50 Bio spectrophotometer.

Starting Materials. Cholester-3-yl-2-methylquinoline-6-yl carbonate (mp 101–102 °C),[46] 6-iodo-2-methylquinoline (mp 108–109 °C),[47] 6-bromo-2-methylquinoline (mp 95–96 °C),[47] cholester-3-yl-*N*-methyl-2-quinaldinium-6-yl carbonate iodide (mp 216–217 °C),[46] 6-iodo-*N*-methyl-2-quinaldinium iodide (mp 222–223 °C),[47] and 6-bromo-*N*-methyl-2-quinaldinium iodide (mp 237 °C)[47] were prepared by modifying the reported procedures. Croconic acid was purchased from Aldrich and used as such. The general synthetic strategy for the croconate dyes **CR-1**−**CR-3** is illustrated in Scheme 3.

Synthesis of the Croconate Dye CR-1. A mixture of the corresponding quinaldinium salt (0.06 mmol), croconic acid (0.03 mmol), and quinoline (0.5 mL) was refluxed in ethanol (6 mL) for 24 h. The solvent was distilled off under reduced pressure to obtain a residue, which was then subjected to column chromatography over silica gel. Elution of the column with a mixture (1:9) of methanol and chloroform gave 75% of the croconate dye **CR-1**; mp 290–292 °C. IR (KBr): ν_{max} (cm^{-1}) 2947, 1755, 1660, 1598, 1560. ^{1}H NMR ($CDCl_3$, 300 MHz): δ 8.99 (2H, d, J = 9.4 Hz), 7.55–7.39 (8H, m), 6.39 (2H, s), 5.37 (2H, s), 4.55 (2H, s), 3.95 (6H, s), 2.44 (4H, s), 1.96–0.75 (82H, m). ^{13}C NMR ($CDCl_3$, 75 MHz): δ 196.6, 188.3, 186.8, 183.2, 154.1, 153.1, 140.4, 130.3, 128.2, 124.9, 123.2, 121.4, 118.2, 117.5, 114.3, 111.1, 108.4, 103.3, 81, 73.3, 72.1, 58.2, 57.7, 51.5, 43.8, 41, 37.7, 37.3, 33.4, 31.2, 30.9, 29.7, 29.5, 25.8, 25.4, 24.4, 24.2, 24.1, 22.6, 20.8, 20.3, 13. FAB-MS: *m/z* Calcd for $C_{83}H_{108}N_2O_7$: 1277.75. Found: 1277.69. Anal. Calcd for $C_{83}H_{108}N_2O_7$: C, 78.02; H, 8.52; N, 2.19. Found: C, 77.85; H, 8.3; N, 2.13.

(26) Das, S.; Thomas, K. G.; Ramanathan, R.; George, M. V.; Kamat, P. V. *J. Phys. Chem.* **1993**, *97*, 13625.
(27) Das, S.; Thanulingam, T. L.; Thomas, K. G.; Kamat, P. V.; George, M. V. *J. Phys. Chem.* **1993**, *97*, 13620.
(28) Das, S.; Kamat, P. V.; de la Barre, B.; Thomas, K. G.; Ajayaghosh, A.; George, M. V. *J. Phys. Chem.* **1992**, *96*, 10327.
(29) Kamat, P. V.; Das, S.; Thomas, K. G.; George, M. V. *J. Phys. Chem.* **1992**, *96*, 195.
(30) Das, S.; Thomas, K. G.; Thomas, J.; George, M. V.; Kamat, P. V. *J. Phys. Chem.* **1994**, *98*, 9291.
(31) Thomas, K. G.; Thomas, K. J.; Das, S.; George, M. V.; Liu, D.; Kamat, P. V. *Faraday Trans.* **1996**, *92*, 4913.
(32) Liu, D.; Kamat, P. V.; Thomas, K. G.; Thomas, K. J.; Das, S.; George, M. V. *J. Chem. Phys.* **1997**, *106*, 6404.
(33) Barazzouk, S.; Lee, H.; Hotchandani, S.; Kamat, P. V. *J. Phys. Chem. B* **2000**, *104*, 3616.
(34) Kamat, P. V.; Das, S.; Thomas, K. G.; George, M. V. *Chem. Phys. Lett.* **1991**, *178*, 75.
(35) Simard, T. P.; Yu, J. H.; Zebrowski-Young, J. M.; Haley, N. F.; Detty, M. R. *J. Org. Chem.* **2000**, *65*, 2236.
(36) Tian, M.; Tatsuura, S.; Furuki, M.; Sato, Y.; Iwasa, I.; Pu, L. S. *J. Am. Chem. Soc.* **2003**, *125*, 348.
(37) Encinas, C.; Otazo, E.; Rivera, L.; Miltsov, S.; Alonso, J. *Tetrahedron Lett.* **2002**, *43*, 8391.
(38) Li, Z. Y.; Jin, Z. H.; Kasatani, K.; Okamoto, H. *Physica B* **2006**, *382*, 229.
(39) Yesudas, K.; Bhanuprakash, K. *J. Phys. Chem. A* **2007**, *111*, 1943.
(40) Prabhakar, Ch.; Yesudas, K.; Chaitanya, K. G.; Sitha, S.; Bhanuprakash, K.; Rao, V. J. *J. Phys. Chem. A* **2005**, *109*, 8604.
(41) Srinivas, K.; Prabhakar, C.; Devi, C. L.; Yesudas, K.; Bhanuprakash, K.; Rao, V. J. *J. Phys. Chem. A* **2007**, *111*, 3378.
(42) Kamat, P. V.; Fox, M. A.; Fatiadi, A. J. *J. Am. Chem. Soc.* **1984**, *106*, 1191.
(43) Kamat, P. V.; Fox, M. A. *J. Electroanal. Chem.* **1983**, *159*, 49.
(44) Hariharan, M.; Joseph, J.; Ramaiah, D. *J. Phys. Chem. B* **2006**, *110*, 24678.
(45) Jyothish, K.; Arun, K. T.; Ramaiah, D. *Org. Lett.* **2004**, *6*, 3965.
(46) Jyothish, K.; Avirah, R. R.; Ramaiah, D. *Org. Lett.* **2006**, *8*, 111.
(47) Jha, B. N.; Banerji, J. C. *Dyes Pigments* **1983**, *4*, 77.

Scheme 3. Synthesis of Croconate Dyes

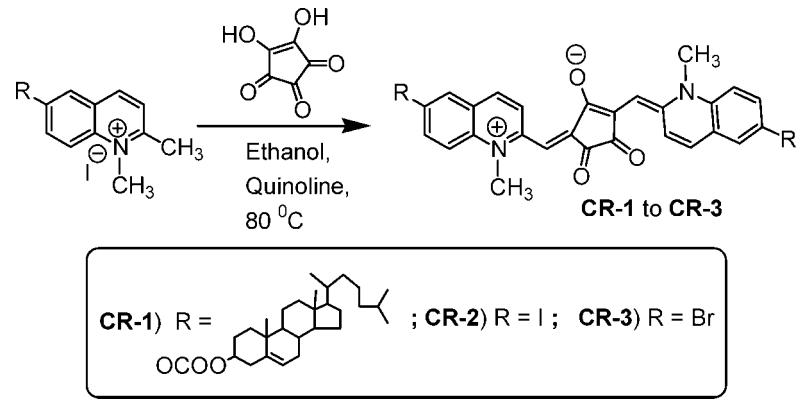

Synthesis of Croconate Dyes CR-2 and CR-3. A mixture of the corresponding quinaldinium salt (0.06 mmol), croconic acid (0.03 mmol), and quinoline (0.5 mL) was refluxed in ethanol (6 mL) for 24 h. The solvent was distilled off under reduced pressure to obtain a residue, which was washed with methanol and DMSO to give the corresponding croconate dyes **CR-2** and **CR-3**.

CR-2 (87%): mp >300 °C. IR (KBr): ν_{max} (cm^{-1}) 3055, 1653, 1606, 1546. FAB-MS: *m*/*z* Calcd for $C_{27}H_{18}I_2N_2O_3$: 672.25. Found: 672.31. Anal. Calcd for $C_{27}H_{18}I_2N_2O_3$: C, 48.04; H, 2.70; N, 4.17. Found: C, 48.21; H, 2.90; N, 4.16.

CR-3 (85%): mp >300 °C. IR (KBr): ν_{max} (cm^{-1}) 3055, 1654, 1608, 1543. FAB-MS: *m*/*z* Calcd for $C_{27}H_{18}Br_2N_2O_3$: 578.25. Found: 579.35. Anal. Calcd for $C_{27}H_{18}Br_2N_2O_3$: C, 56.08; H, 3.14; N, 4.84. Found: C, 55.74; H, 2.97; N, 5.10.

SnO_2 Electrodes (OTE/SnO_2). The SnO_2 (15%) suspension obtained from Alfa Chemicals was first diluted (1 mL of SnO_2 solution with 47 mL of water and 2 mL of ammonium hydroxide) to obtain 0.3% solution. 500 μL of this diluted suspension was spread over 2 cm^2 area of an optically transparent electrode (OTE). These electrodes were then air-dried on a warm plate and annealed in an oven at 673 K for 1 h. Details on the preparation of electrodes can be found elsewhere.[48]

TiO_2 Electrodes (OTE/TiO_2). TiO_2 colloids were first prepared by hydrolyzing titanium isopropoxide in glacial acetic acid solution followed by autoclaving the suspension at 507 K for 12 h. The details of the procedure can be found elsewhere.[49] 500 μL of the suspension was spread over the OTE plate using a syringe. After air drying the electrodes were annealed in an oven at 673 K for 1 h.

Transient Absorption Spectroscopy. Ultrafast (femtosecond) transient absorption experiments were conducted using a Clark-MXR 2010 laser system and an optical detection system provided by Ultrafast Systems (Helios). The source for the pump and probe–pulses is the fundamental of the Clark laser system (775 nm, 1 mJ/pulse, fwhm 130 fs, 1 kHz repetition rate). 5% of the output is used to generate a white light continuum probe pulses. Prior to creating the white light probe, the fundamental is fed through a delay line providing an experimental time window of 1.6 ns with a maximum step resolution of 7 fs. The pump beam is attenuated to 5 μJ/pulse with a spot size of 2 mm (diameter) at the sample where it is merged with the white light incident on the sample cell with an angle <10°. After passing through the samples, the probe is focused onto a 200 μm core fiber connected to a CCD spectrograph (Ocean Optics, S2000-UV-vis (425–800 nm), or Sensors Unlimited, SU-LDV-512LDB (750–1200 nm)), enabling time-resolved spectra to be recorded. Typically, 5000 excitation pulses are averaged to obtain the transient spectrum at a set delay time. Kinetic traces at appropriate wavelengths are assembled from the time-resolved data. All measurements were conducted at room temperature.

Nanosecond laser flash photolysis experiments were performed with a 355 nm laser pulse (5 mJ, pulse width 6 ns) from a Quanta Ray Nd:YAG laser system. The experiments were performed in a rectangular quartz cell, and all the solutions were deaerated with high-purity argon.

Photoelectrochemical Measurements. Photoelectrochemical measurements were performed using a standard two-compartment cell consisting of a working electrode and Pt wire gauze counter electrode. All photoelectrochemical measurements were carried out in acetonitrile containing 0.5 M LiI and 0.05 M I_2. Photocurrents were measured using a Keithley model 2601 source meter. A collimated light beam from a 150 W xenon lamp with a 400 nm cutoff filter was used for excitation of the electrodes. A Bausch and Lomb high-intensity grating monochromator was introduced into the path of the excitation beam for selecting appropriate wavelength. The incident photon-to-photocurrent efficiency (IPCE) at various excitation wavelengths was determined from the eq 1

$$\text{IPCE}\ (\%) = \frac{i_{sc}}{I_{inc}} \frac{1240}{\lambda} \times 100 \qquad (1)$$

where i_{sc} is the short-circuit photocurrent (A/cm^2), I_{inc} is the incident light intensity (W/cm^2), and λ is the excitation wavelength.

Results and Discussion

Absorption Properties of Ground and Excited Dye Molecules. The synthesis of the croconate dyes **CR-1**, **CR-2**, and **CR-3** (Scheme 2) has been achieved in good yields (75–87%) through the condensation reaction between croconic acid and the corresponding quinaldinium salts in 2:1 equivalents in ethanol. As explained in the Experimental Section, these dyes were purified and characterized on the basis of spectral data and analytical evidence. These three symmetrical croconate dyes chosen in this study contain same central acceptor moiety but vary in attached donor groups. Dyes **CR-2** and **CR-3** are soluble only in DMF. **CR-1**, on the other hand, is soluble in most of the solvents such as $CHCl_3$, THF, CH_2Cl_2, etc., thus giving flexibility in its photochemical and photoelectrochemical characterization. All three dyes exhibit similar absorption features with maximum

(48) Bedja, I.; Hotchandani, S.; Kamat, P. V. *J. Phys. Chem.* **1994**, *98*, 4133.
(49) Subramanian, V.; Wolf, E. E.; Kamat, P. V. *J. Am. Chem. Soc.* **2004**, *126*, 4943.

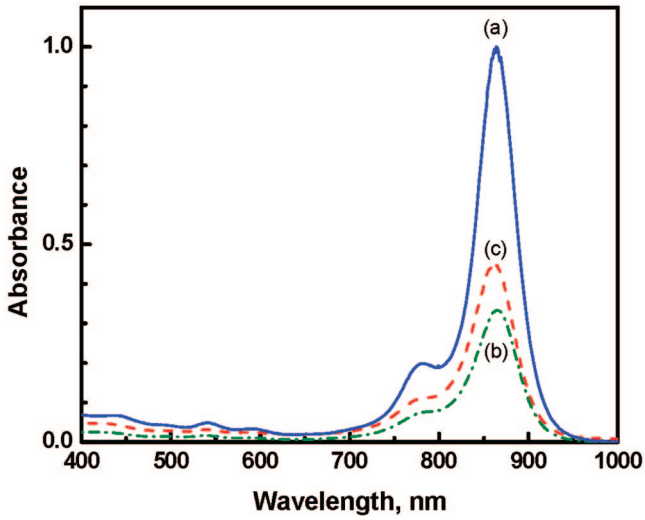

Figure 1. Absorption spectra of 2.4 μM croconate dyes: (a) **CR-1** in $CHCl_3$, (b) **CR-2** in DMF, and (c) **CR-3** in DMF.

Table 1. Excited-State Properties of Croconate Dyes

dye	solvent	abs max λ_{max} (nm)	ext coeff at λ_{max} (M^{-1} cm^{-1})	S_1-S_n abs max (nm)	excited singlet lifetime (ps)
CR-1	$CHCl_3$	865	4.2×10^5	630, 720	7.3
CR-2	DMF	865	1.4×10^5	635, 685	4.4
CR-3	DMF	861	1.9×10^5	630, 720	4.1

around 865 nm (Figure 1). The similarity in the absorption features indicates that the side-chain groups have minimal effect on the absorption properties. These dyes are nonfluorescent, and hence their singlet excited-state characterization using emission spectroscopy is difficult. We employed femtosecond transient absorption spectroscopy to probe the excited-state behavior of croconate dyes. The absorption properties are summarized in Table 1.

The time-resolved spectra of the transients recorded following 775 nm laser pulse excitation of croconate dye **CR-1** in methylene chloride are shown in Figure 2. The formation of the singlet excited state can be seen from the transient absorption spectrum recorded immediately after 130 fs laser pulse excitation. The difference absorption spectrum shows a broad absorption peak in the visible with split maxima at 630 and 720 nm. The decay of this absorption band in the visible parallels the bleaching recovery at 860 nm. The excited-state lifetime as monitored from the decay at 630 nm is 7.3 ps.

The transient absorption spectra recorded after excitation of **CR-2** and **CR-3** are shown in the Supporting Information (Figures S1 and S2). The excited singlets of these two dyes also show similar broad absorption in the 600–720 nm and exhibit lifetimes of 4.4 and 4.1 ps in dimethylformamide, respectively. The decreased lifetime of these two dye singlets compared to **CR-1** is expected to arise from the difference in the solvent medium. As described earlier, the excited-state properties of squaraine and croconate dyes are strongly dependent on the polarity of the solvent.[41] Limited solubility of the dyes in different solvents restricted detailed evaluation of medium effects.

It is interesting to note that the bleaching recovery for all three dyes is completed within ~40 ps. This complete recovery of the ground state in turn indicates the absence of long-lived transients and confirms that singlet excited state is the only transient formed when monomer croconate dye is excited with 775 nm laser pulse. Absence of long-lived transient rules out the possibility of intersystem crossing in the formation of triplet excited state. The side-chain modification with Br, I, or cholesterol group had little effect on the formation or deactivation of the croconate singlet excited state. In the forgoing studies we have chosen **CR-1** dye as the representative dye to explore the light harvesting properties.

Generation of Triplet Excited State via T−T Energy Transfer. Since the intersystem crossing efficiency was negligible under direct excitation of the dye, we adopted a triplet–triplet (T−T) energy-transfer method to characterize the triplet excited state of the croconate dye. A similar energy-transfer method has been used to characterize the triplet excited state of squaraine dyes.[50] Pyrenecarboxaldehyde, **PyC** (E_T = 186 kcal/mol; λ_{max} = 440 nm and ϵ_{max} = 20000 M^{-1} cm^{-1}), in dichloromethane was used as a sensitizer to transfer triplet energy to **CR-1** in a nanosecond laser flash photolysis set up (reactions 2 and 3).

$$\mathrm{PyC} + h\nu \rightarrow {}^1\mathrm{PyC}^* \xrightarrow{\mathrm{ISC}} {}^3\mathrm{PyC}^* \qquad (2)$$

$${}^3\mathrm{PyC}^* + \mathrm{dye} \rightarrow \mathrm{PyC} + {}^3\mathrm{dye}^* \qquad (3)$$

The transient absorption spectrum recorded immediately after 355 nm laser pulse excitation of **PyC** shows absorption maximum at 440 nm, corresponding to the triplet excited state (spectrum a in Figure 3). In the presence of **CR-1**, the deactivation of the pyrene triplet proceeds via T−T energy transfer, as illustrated by reaction 2. This is evident from the growth of a new absorption band in the visible region (spectra b and c in Figure 3). The broad absorption band seen around 500 and 680 nm corresponds to the triplet **CR-1**. The bimolecular rate constant as determined from the dependence of pseudo-first-order decay rate constant of **PyC** triplet on the concentration of **CR-1** is 1.8×10^{10} M^{-1} s^{-1}. If we assume energy transfer to be 100%, we can determine the extinction coefficient of triplet excited **CR-1**. By comparing the maximum absorbance values and the extinction coefficient of **PyC** triplet, we obtain a value of 15500 M^{-1} cm^{-1} for **CR-1** triplet at 680 nm. The triplet excited **CR-1** is relatively long-lived (lifetime of 7.2 μs) compared to its singlet excited state (7.3 ps). Spectrum d in Figure 3 shows the residual absorption following the decay of triplet excited state. The formation of the photoproduct is an indication of the photochemical reactivity of the triplet excited state. Since the triplet excited state has a long life, if formed under direct excitation, we could have seen as a long-lived transient in Figure 2. These results further ascertain our earlier conclusion that the intersystem crossing is a minor pathway in the deactivation of the singlet excited state.

Absorption Properties of Croconate Dye Films. One way to utilize the croconate dyes for harvesting infrared

(50) Sauve, G.; Kamat, P. V.; Thomas, K. G.; Thomas, J.; Das, S.; George, M. V. *J. Phys. Chem.* **1996**, *100*, 2117.

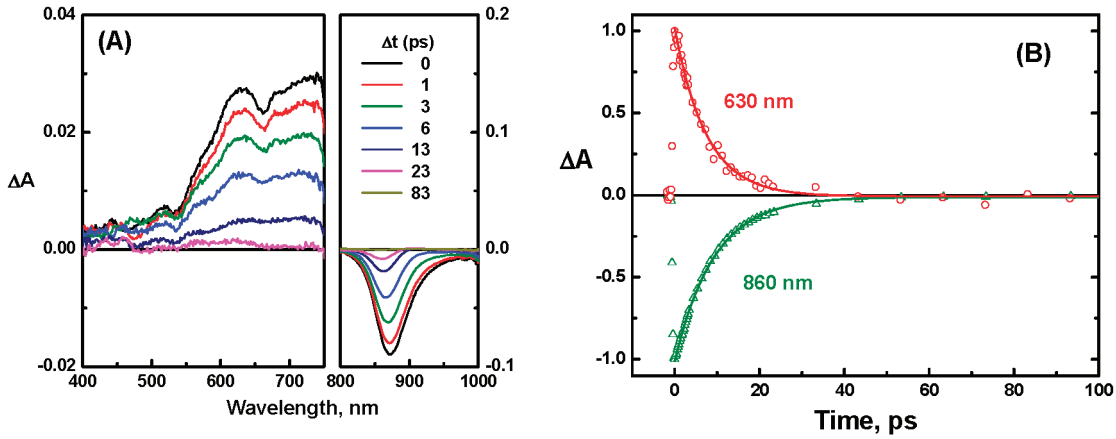

Figure 2. Transient absorption spectra recorded following the 775 nm laser pulse excitation of **CR-1** in CH_2Cl_2: (A) time-resolved absorption spectra recorded at 0, 1, 3, 6, 13, 23, and 83 ps; (B) absorption−time profiles recorded at 630 and 860 nm. (The maximum absorbance is normalized to 1 and –1, respectively.)

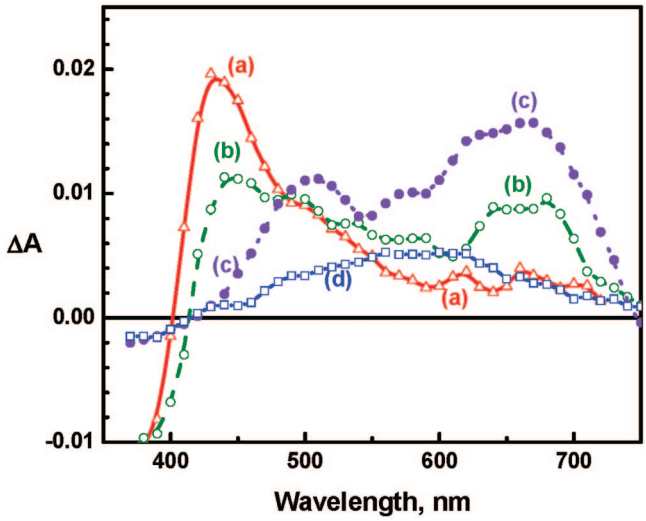

Figure 3. T−T energy transfer between excited 0.1 mM **PyC** and 0.02 mM **CR-1** in dichloromethane. Time-resolved spectra were recorded following 355 nm laser pulse excitation: (a) 50 ns, (b) 500 ns, (c) 5 μs, and (d) 20 μs.

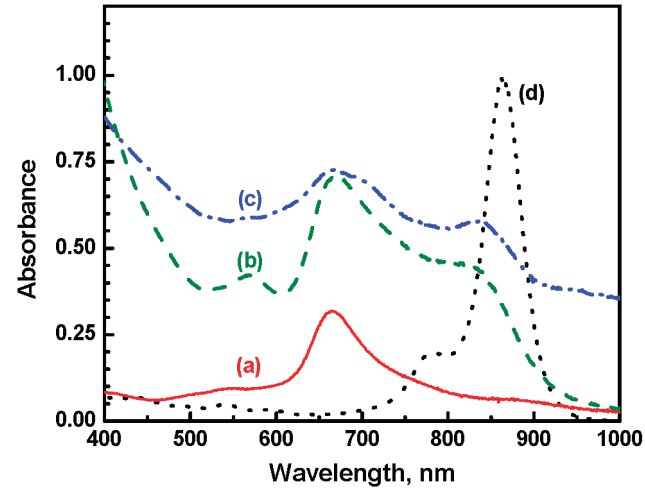

Figure 4. Absorption spectra of the croconate dye **CR-1** cast or deposited on (a) glass slide using the drop-cast method, (b) nanostructured TiO_2 film, and (c) nanostructured SnO_2 film using the dip-adsorption method. The monomer solution spectrum (d) is also shown for comparison.

photons (e.g., in a photoelectrochemical cell) is to cast thin films on the electrode surface. We have employed two different approaches for casting the films of **CR-1**. A drop-cast method was employed to cast thin film of **CR-1** on glass slide by applying the chloroform solution and air-drying. A dip-adsorption method was employed to assemble the dye film on nanostructured TiO_2 and SnO_2 films. The electrodes with SnO_2 and TiO_2 films were immersed in a chloroform solution of 0.1 mM **CR-1** solution for 12 h. The change in the color of the film shows adsorption of the dye through noncovalent interactions. The absorption spectra of the dye film cast on conducting glass and the dye molecules deposited on TiO_2 and SnO_2 films are shown in Figure 4.

Compared to the absorption band of the monomer form, the dye film cast on the conducting glass exhibits a blue-shifted absorption band with a maximum at 660 nm. This absorption is indicative of H-aggregate formation as the dye molecules are assembled in an organized fashion. Formation of such aggregates in the films and heterogeneous media is commonly seen for IR dyes.[23,24,27,33,51] It is interesting to note that the dye molecules adsorbed on the nanostructured TiO_2 and SnO_2 films exhibit additional peaks compared to the film obtained by the drop-cast method. The presence of both monomer and aggregate forms is evident from the absorption spectra b and c in Figure 4. The presence of smaller peaks in the higher energy region (e.g., 560 nm) is indicative of higher ordered aggregates such as the trimer of **CR-1**. The broadness of the aggregation peak indicates the degree of randomness of the aggregates formed in these films. As compared to the solution spectrum, the absorption peak of the monomer dye on TiO_2 and SnO_2 surface is slightly blue-shifted with a maximum around 840 nm. (Note that the SnO_2 film is semitransparent, and the absorption has not been corrected for scattering effects. The long-wavelength absorption (>900 nm) in these films arises from scattering effects.) The presence of monomer form in these films indicates that the surface of the oxide particles promotes dispersion of dye molecules without aggregation.

(51) Das, S.; Thomas, J.; Thomas, K. G.; Madhavan, V.; Liu, D.; Kamat, P. V.; George, M. V. *J. Phys. Chem.* **1996**, *100*, 17310.

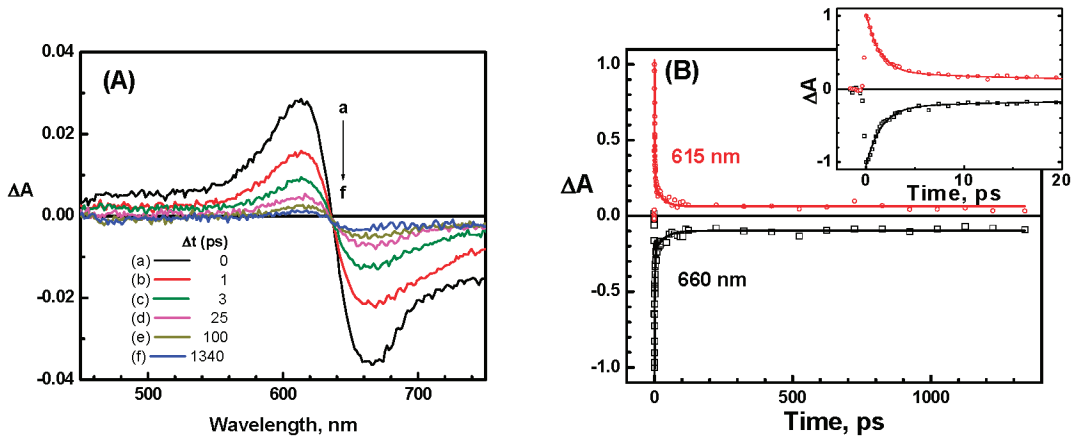

Figure 5. Transient absorption spectra recorded following the 775 nm laser pulse excitation of **CR-1** film on glass: (A) time-resolved absorption spectra recorded at 0, 1, 3, 25, 100, and 1340 ps; (B) absorption−time profiles recorded at 615 and 660 nm. (Inset shows the decay and recovery profiles at short time scales with absorption values normalized to unity.)

The excited-state behavior of croconate dye films was further investigated using pump–probe spectroscopy. Figure 5 shows the time-resolved absorption spectra recorded following 775 nm excitation of **CR-1** film cast on a conducting glass electrode. A difference absorption peak at 610 nm and bleaching at 670 nm can be seen as the excitonic state of the dye aggregate is generated following infrared laser excitation. The transient decay, when fitted to biexponential decay analysis, gave lifetime values of 1.1 and 7.6 ps. The inhomogeneity of the aggregates in the film is expected to influence the decay kinetics and contribute to the deviation from the monoexponential decay behavior.

The excited singlet of H-aggregate is nonfluorescent because of the forbidden transition between the lower excited singlet level and ground state.[52,53] Thus, excited H-aggregates undergo intersystem crossing to produce relatively long-lived triplet species. In our earlier studies we have characterized the triplet properties of cyanine,[33] thiazine,[54] and oxazine dye[55,56] aggregates. In the present study we find that more than 98% of the bleached dye is recovered in ~30 ps. On the basis of this observation, we can conclude that the intersystem crossing is not a dominant deactivation pathway for the excited dimer of **CR-1**. We can further conclude that the excited state or excitonic state formed with direct excitation of the dye aggregate on a glass surface undergoes rapid annihilation without producing charge-separated state or triplet excited state. In order to see whether the semiconducting property of TiO_2 and SnO_2 can influence the charge separation process, we evaluated the transient spectra following laser pulse excitation of **CR-1** films.

Figure 6 compares the transient spectra recorded following the 387 nm laser pulse excitation of the **CR-1** film on glass and TiO_2 surface. The higher energy of the laser pulse (compared to the 775 nm laser pulse in Figure 5) chosen for this experiment ensured the excitation of all aggregated forms of the dye in the film. Neither the SnO_2 nor TiO_2 (E_g > 3.5 eV) substrate can be directly excited with 387 nm laser pulse. The transient absorption and decay behavior of the **CR-1** film on the glass surface was similar to the one observed with 775 nm laser pulse excitation. Any higher energy states formed during 387 nm laser pulse excitation are quickly relaxed to form the excitonic state similar to the 775 nm laser pulse excitation. The transient decay deviates from the monoexponential behavior. The biexponential kinetic analysis of the transient decay yielded lifetimes of 1 and 11 ps.

Interestingly, we observe a different type of transient absorption behavior on the TiO_2 surface with a broad maximum around 500 nm. The bleaching in the 670 nm confirms that the origin of the transient is still centered on the dimer of **CR-1**. Upon fitting the transient decay at 500 nm to biexponential kinetic analysis, we obtain lifetimes of 0.5 and 3.4 ps. A similar result was also obtained on the surface of SnO_2 (see Figure S3, Supporting Information). The transient absorption at 500 nm was predominant and decayed with a lifetime of 0.2 and 7.0 ps.

Two notable differences emerge from these experiments. (i) The transient observed on the TiO_2 and SnO_2 surface exhibits blue-shifted absorption compared to the excitonic absorption on the glass surface. (ii) The initial decay times of the transient on the TiO_2 and SnO_2 surface are shorter than the one observed on the glass surface, and formation of the long-lived transient is also visualized from the residual bleaching at 690 nm. These results suggest that a significant fraction of the excitonic state of the aggregate dye dissociates at the TiO_2 surface to generate the charge-separated pair. We attribute the transient absorption around 500 nm to this charge-separated state. Whereas most of these separated charges undergo recombination, a small fraction (<10%) of the charge-separated state is stabilized as the electrons are trapped within the TiO_2 particles. The possible reaction pathways with which the excited dye aggregates in the film undergo deactivations are summarized in reactions 4−7.

$$(\text{dye})_2 + h\nu \rightarrow (\text{dye})_2{}^* \quad (4)$$

$$(\text{dye})_2{}^* \rightarrow (\text{dye})_2 \quad (5)$$

$$(\text{dye})_2{}^* \rightarrow (\text{dye}^+ - \text{dye}^-) \rightarrow (\text{dye})_2 \quad (6)$$

$$(\text{dye}^+ - \text{dye}^-) + \text{TiO}_2 \rightarrow (\text{dye}^+ - \text{dye}) + \text{TiO}_2(\text{e}) \quad (7)$$

If indeed TiO_2 is capable of accepting electrons from the charge-separated dye aggregate, we should be able to collect

(52) McRae, E. G.; Kasha, M. *J. Chem. Phys.* **1958**, *28*, 721.
(53) Kasha, M.; Rawls, H. R.; El-Bayoumi, M. A. *Pure Appl. Chem.* **1965**, *11*, 371.
(54) Das, S.; Kamat, P. V. *J. Phys. Chem. B* **1999**, *103*, 209.
(55) Liu, D.; Hug, G. L.; Kamat, P. V. *J. Phys. Chem.* **1995**, *99*, 16768.
(56) Liu, D.; Kamat, P. V. *J. Chem. Phys.* **1996**, *105*, 965.

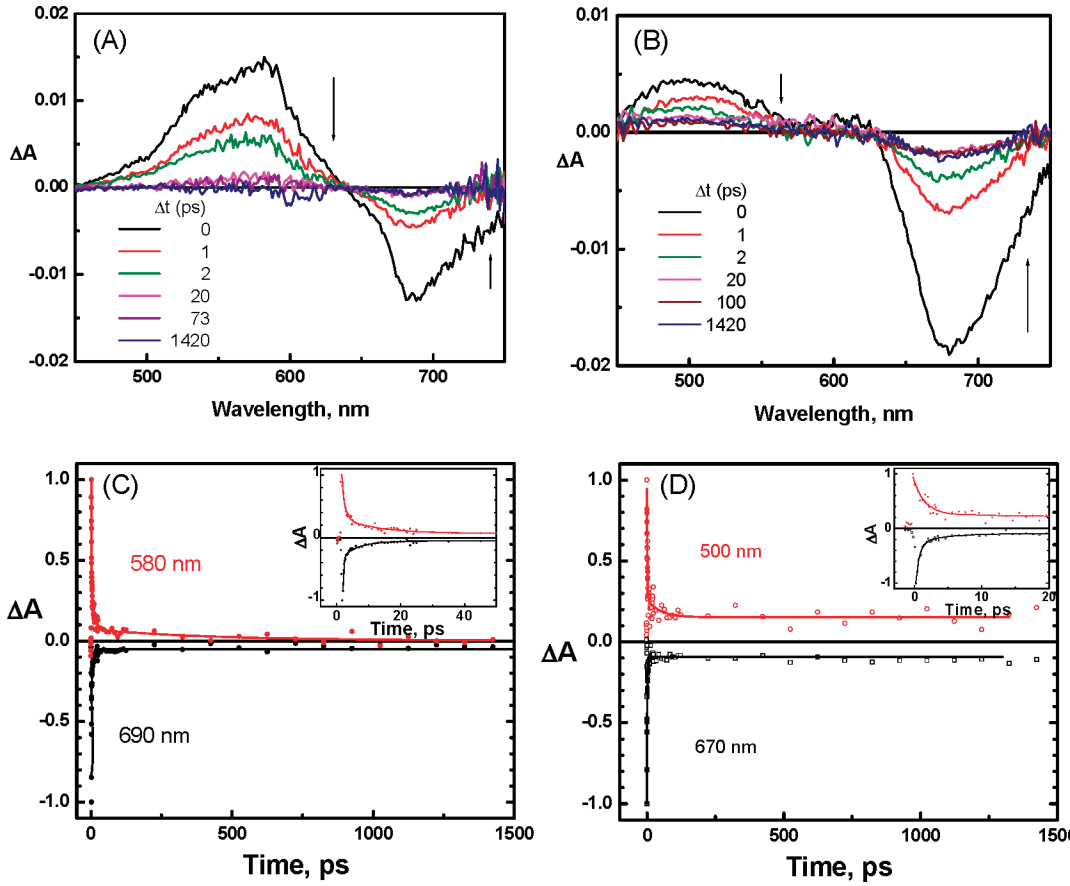

Figure 6. Transient absorption spectra recorded following the 387 nm laser pulse excitation of **CR-1** film on (A) glass and (B) nanostructured TiO_2 film. The absorption−time profiles recorded for (C) **CR-1** film on glass at 580 and 690 nm and (D) nanostructured TiO_2 film at 500 and 670 nm.

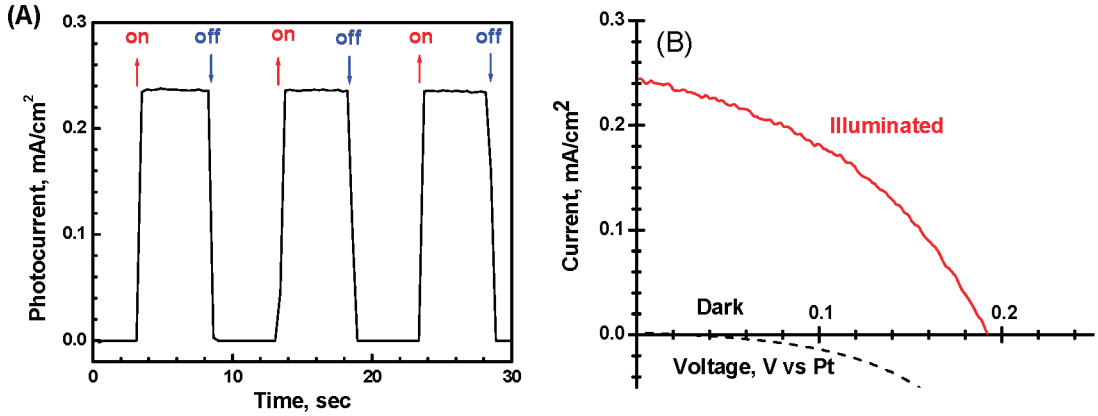

Figure 7. (A) Photocurrent response and (B) power characteristics of OTE/TiO_2/**CR-1** electrode. Excitation: >400 nm, 100 mW/cm^2. Electrolyte: 0.5 M LiI and 0.05 M I_2 in acetonitrile.

these charges at the electrode surface in a photoelectrochemical cell.

Photocurrent Generation at Croconate Dye-Modified TiO_2 Electrode. The nanostructured TiO_2 film was first cast on a conducting glass electrode (OTE/TiO_2) using TiO_2 colloids. The **CR-1** dye deposited on the TiO_2 surface (referred as OTE/TiO_2/**CR-1**) is photoactive and generates photocurrent in a photoelectrochemical cell when subjected to light irradiation. Figure 7 shows the photocurrent response to on–off cycles of illumination and the power characteristics of the cell. The photocurrent response is prompt and reproducible at several cycles of illumination. As the electrons are transported toward the collecting electrode surface, the dye is regenerated by the redox couple (I_3^-/I^-) at the electrolyte interface. We observe a maximum current of 0.23 mA/cm^2 and a photovoltage of 190 mV for visible−IR illumination (100 mW/cm^2) of the electrode. Although overall power conversion efficiency is small (<0.1%), the generation of anodic photocurrent confirms the light-initiated electron flow toward TiO_2 film and the collecting OTE surface.

We also evaluated the incident photon to charge carrier generation efficiency (IPCE) of OTE/TiO_2/**CR-1** electrode (Figure 8) and OTE/SnO_2/**CR-1** electrode (see Figure S5, Supporting Information). The experiments were carried out in a two-arm flat cell, and the illumination area was limited to 0.28 cm^2. The **CR-1**-modified OTE/TiO_2 electrode shows photocurrent response in the 500–800 nm region, thus matching

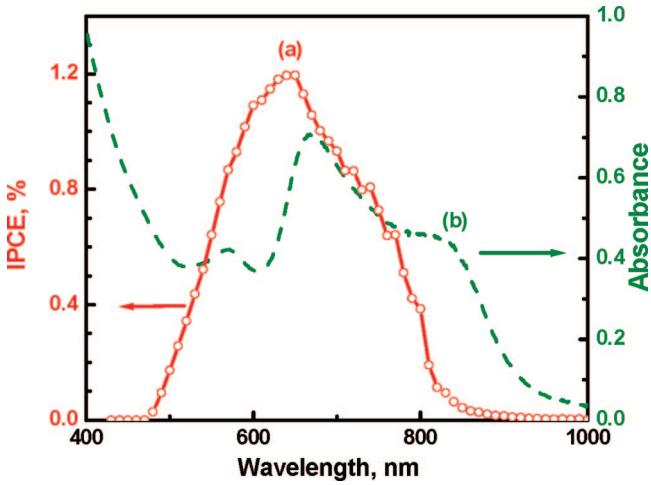

Figure 8. Photocurrent response of OTE/TiO_2/**CR-1** electrode to monochromatic illumination. The comparison of (a) IPCE and (b) absorbance traces shows the primary species responsible for photocurrent generation. Electrolyte: 0.5 M LiI and 0.05 M I_2 in acetonitrile.

the absorption of the H-aggregates. The maximum IPCE was ~1.2% (curve a) at 650 nm. The performance of the OTE/SnO_2/**CR-1** electrode was relatively poor with a maximum IPCE of 0.6%. It is interesting to note that the IPCE at longer wavelengths (>800 nm) is relatively low, and there was no contribution from the monomeric dye to the photocurrent generation. The blue shift in the IPCE peak compared to the absorption maximum is indicative of the fact that higher aggregates of **CR-1** contribute to the photocurrent generation with greater efficiency. The varying photocurrent generation efficiency of monomers vs aggregates has been elucidated in earlier studies.[57–60] Compared to **CR-1**, other croconate dyes, **CR-2** and **CR-3**, performed poorly, and no attempt was made to further evaluate the photoelectrochemical performance of these two dyes. (In order to probe the photoelectrochemical response in the visible region, we have used 475 nm cutoff filters for photocurrent measurements. Hence, the photoelectrochemical response below 500 nm is not represented accurately in Figure 8.)

In recent years extensive effort has been made to sensitize TiO_2 using various dyes.[61] In a dye-sensitized photocurrent generation mechanism, the excited singlet of the sensitizing dye directly injects electrons into the TiO_2 particles. The oxidation potential of the ground-state dye (**CR-1**) as determined from the cyclic voltammetry experiment is 1.22 V vs NHE (see Figure S4, Supporting Information). This value corresponds to ~−0.23 V for the oxidation potential of the excited monomer (assuming the singlet energy as 1.45 eV). Since the conduction band energy of TiO_2 (−0.5 V vs NHE) is more negative than the oxidation potential, the excited monomer form of the dye cannot directly participate in the charge injection process. As a result of this energy mismatch, we are not able to observe sensitized photocurrent generation from the **CR-1** monomer. However, the dye aggregates are capable of generating photocurrent as the excitons undergo charge separation and thus contribute to the photocurrent.[62] In the present study we have not explored the role of deoxycholic acid substituent in directing the adsorption of dye molecules on oxide surface. Such substituents can play a major role in the assembly of dye molecules on the oxide surfaces. For example, it has been used as a coadsorbate on the electrode surface to improve the photovoltaic performance in dye-sensitized solar cells.[63]

The photoelectrochemical experiments illustrated in the present study show the ability of TiO_2 (or SnO_2) to capture the electrons and transport them to the OTE collecting surface. However, the overall photocurrent conversion efficiency remains rather low. As demonstrated in the transient absorption experiments, the major fraction of the charge-separated pair undergoes recombination. Strategies to use conducting polymer layers for improving the interaction with organic molecules have been found useful in enhancing the performance of organic LED.[64,65] Such approaches need to be exploited in the construction of organic dye-based solar cells.

Conclusions

The photophysical properties of croconate dyes in the monomeric and aggregated forms have been characterized using femtosecond spectroscopy. The singlet excited state of the monomer is short-lived (7.3 ps) and does not undergo intersystem crossing to produce long-lived triplet. The excitation of the H-aggregate produces excitons which are capable of undergoing charge separation on the TiO_2 and SnO_2 surface. When the dye molecules adsorbed on TiO_2 films were excited with visible−IR light, we observe anodic current generation. Only the aggregates contribute to the photocurrent generation. The low IPCE of croconate dye film shows that the net charge separation is poor. Improvement in the dye aggregate/semiconductor heterojunction is necessary to further improve the efficiency of charge separation.

Acknowledgment. The research described herein was supported by the Office of Basic Energy Science of the Department of the U.S. Department of Energy. D.R., R.R.A., and K.J. acknowledge the Council of Scientific and Industrial Research (CSIR) and Department of Science and Technology, Government of India, for financial support. We also thank Toyota Central R&D Labs., Inc., Aichi, Japan, for the research grant for enabling T.K. stay at Notre Dame. This is contribution NDRL 4737 from the Notre Dame Radiation Laboratory.

Supporting Information Available: Transient absorption spectra of **CR-1**, **CR-2**, and **CR-3**, cyclic voltammogram of **CR-1**, and photocurrent response of OTE/SnO_2/**CR-1**. This material is available free of charge via the Internet at http://pubs.acs.org.

CM7018668

(57) Khazraji, A. C.; Hotchandani, S.; Das, S.; Kamat, P. V. *J. Phys. Chem. B* **1999**, *103*, 4693.
(58) Natoli, L. M.; Ryan, M. A.; Spitler, M. T. *J. Phys. Chem.* **1985**, *89*, 1448.
(59) Sayama, K.; Tsukagoshi, S.; Hara, K.; Ohga, Y.; Shinpou, A.; Abe, Y.; Suga, S.; Arakawa, H *J. Phys. Chem. B* **2002**, *106*, 1363.
(60) Toerne, K.; von Wandruszka, R. *Langmuir* **2002**, *18*, 7349.
(61) Meyer, G. J. *Inorg. Chem.* **2005**, *44*, 6852.
(62) Gregg, B. A. *J. Phys. Chem. B* **2003**, *107*, 4688.
(63) He, J. J.; Benko, G.; Korodi, F.; Polivka, T.; Lomoth, R.; Akermark, B.; Sun, L. C.; Hagfeldt, A.; Sundstrom, V. *J. Am. Chem. Soc.* **2002**, *124*, 4922.
(64) Marrikar, F. S.; Brumbach, M.; Evans, D. H.; Lebron-Paler, A.; Pemberton, J. E.; Wysocki, R. J.; Armstrong, N. R. *Langmuir* **2007**, *23*, 1530.
(65) Carter, C.; Brumbach, M.; Donley, C.; Hreha, R. D.; Marder, S. R.; Domercq, B.; Yoo, S.; Kippelen, B.; Armstrong, N. R. *J. Phys. Chem. B* **2006**, *110*, 25191.